Spatial variations in slip rate along the Death Valley-Fish Lake Valley fault system determined from LiDAR topographic data and cosmogenic ^{10}Be geochronology

Kurt L. Frankel,[1,2] James F. Dolan,[1] Robert C. Finkel,[3] Lewis A. Owen,[4] and Jeffrey S. Hoeft[1,5]

Received 8 May 2007; revised 25 June 2007; accepted 11 July 2007; published 19 September 2007.

[1] The Death Valley-Fish Lake Valley fault zone (DV-FLVFZ) is a prominent dextral fault system in the eastern California shear zone (ECSZ). Combining offset measurements determined with LiDAR topographic data for two alluvial fans with terrestrial cosmogenic nuclide ^{10}Be ages from the fan surfaces yields a late Pleistocene slip rate of ~2.5 to 3 mm/yr for the northern part of the DV-FLVFZ in Fish Lake Valley. These rates are slower than the late Pleistocene rate determined for the system in northern Death Valley, indicating that slip rates decrease northward along this major fault zone. When summed with the slip rate from the White Mountains fault, the other major fault in this part of the ECSZ, our results suggest that either significant deformation is accommodated on structures east of Fish Lake Valley, or that rates of seismic strain accumulation and release have not remained constant over late Pleistocene to Holocene time. **Citation:** Frankel, K. L., J. F. Dolan, R. C. Finkel, L. A. Owen, and J. S. Hoeft (2007), Spatial variations in slip rate along the Death Valley-Fish Lake Valley fault system determined from LiDAR topographic data and cosmogenic ^{10}Be geochronology, *Geophys. Res. Lett.*, *34*, L18303, doi:10.1029/2007GL030549.

1. Introduction

[2] The degree to which fault loading and strain release rates are constant in time and space is one of the most fundamental, unresolved issues in modern tectonics. In particular, data concerning the manner in which strain is distributed across plate boundaries in time and space are necessary to understand the complex behavior of plate boundary fault systems and the lithospheric deformation that they accommodate. Such analyses require a comparison of slip rate data over a wide range of temporal and spatial scales.

[3] The Death Valley-Fish Lake Valley fault zone (DV-FLVFZ) is thought to accommodate much of the relative Pacific-North America plate motion east of the San Andreas fault (Figure 1). Although numerous geodetic campaigns have addressed issues of strain accumulation along this part of the plate boundary [e.g., *Dixon et al.*, 1995, 2000, 2003; *Bennett et al.*, 2003, and references therein], only a few field-based studies have attempted to measure longer-term (1,000 to 100,000 year) geologic slip rates along this fault system [*Brogan et al.*, 1991; *Reheis and Sawyer*, 1997; *Frankel et al.*, 2007]. The relative scarcity of field-based studies utilizing quantitative geochronologic techniques to investigate deformational processes over millennial to million-year time scales has made it difficult to assess the behavior of the plate boundary in the region.

[4] Here, we use a multidisciplinary approach that encompasses analysis of high-resolution LiDAR digital topographic data combined with terrestrial cosmogenic nuclide (TCN) ^{10}Be geochronology to determine late Pleistocene slip rates along the northern part of the DV-FLVFZ in Fish Lake Valley (FLV). Our results reveal spatial variations in strain release rates along the DV-FLVFZ that have important implications for understanding the dynamics of Pacific-North America plate boundary deformation within the ECSZ.

2. Eastern California Shear Zone Kinematics

[5] The ECSZ and its northern continuation, the Walker Lane belt, extend for >800 km through the Mojave Desert and northward along the western edge of the Basin and Range. This system of predominantly right-lateral faults (Figure 1) is thought to accommodate 9.3 ± 0.2 mm/yr (~20%) of elastic strain accumulation along Pacific-North America plate boundary [*Bennett et al.*, 2003]. Displacement from the Mojave segment of the ECSZ is funneled northward across the Garlock fault onto the Owens Valley, Panamint Valley-Hunter Mountain-Saline Valley, Death Valley-Fish Lake Valley, and Stateline fault zones (Figure 1). A number of northeast-trending faults transfer slip between the faults of Owens and Panamint Valleys and the DV-FLVFZ (Figure 1) [*Dixon et al.*, 1995; *Reheis and Dixon*, 1996; *Lee et al.*, 2001]. Farther north, dextral motion between the Sierra Nevada block and North America is focused on two faults bounding the White Mountains: the White Mountains fault zone (WMFZ) to the west and the DV-FLVFZ to the east. Modeling of GPS data suggests the DV-FLVZ is storing strain at a rate of 4 to 10 mm/yr, while the WMFZ stores strain at 1 to 5 mm/yr [*Dixon et al.*, 1995, 2000]. Thus, at latitude 37.5°N, geodetic data suggest that almost all plate-boundary deformation east of the SAF is accommodated on the WMFZ and northern part of the DV-FLVFZ.

[1]Department of Earth Sciences, University of Southern California, Los Angeles, California, USA.
[2]Now at School of Earth and Atmospheric Sciences, Georgia Institute of Technology, Atlanta, Georgia, USA.
[3]Center for Accelerator Mass Spectrometry, Lawrence Livermore National Laboratory, Livermore, California, USA.
[4]Department of Geology, University of Cincinnati, Cincinnati, Ohio, USA.
[5]Now at William Lettis & Associates, Inc., Walnut Creek, California, USA.

0094-8276/07/2007GL030549$05.00

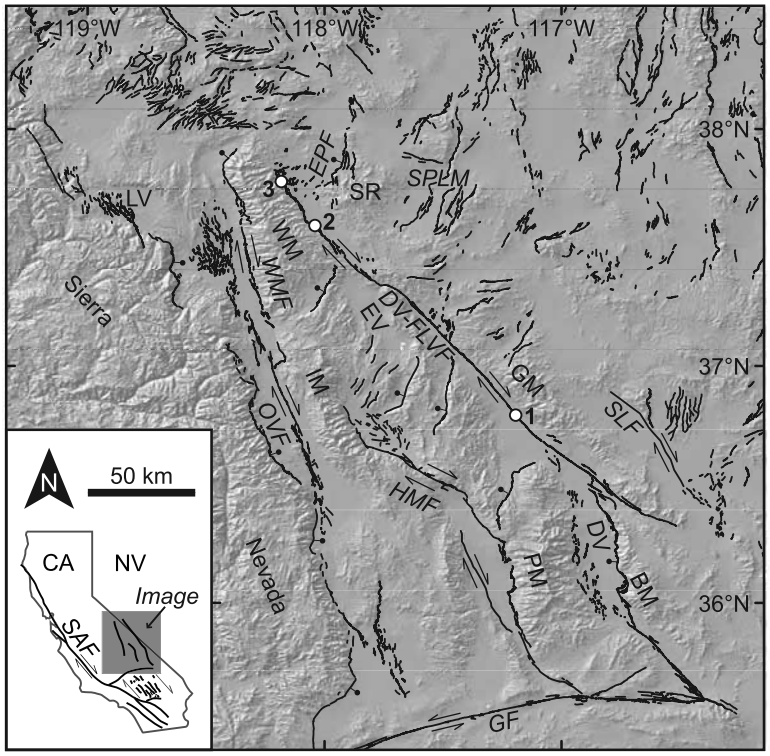

Figure 1. Map of topography and Quaternary faults in the northern ECSZ. 1, Red Wall Canyon alluvial fan; 2, Furnace Creek alluvial fan (Figure 2); 3, Indian Creek alluvial fan (Figure 3). GF, Garlock fault; BM, Black Mountains; DV, Death Valley; PM, Panamint Mountains; HMF, Panamint Valley-Hunter Mountain-Saline Valley fault zone; OVF, Owens Valley fault zone; DV-FLVF, Death Valley-Fish Lake Valley fault zone; IM, Inyo Mountains; GM, Grapevine Mountains; SLF, Stateline fault zone; EV, Eureka Valley; WMF, White Mountains fault zone; WM, White Mountains; EPF, Emigrant Peak fault zone; LV, Long Valley caldera; SR, Silver Peak Range; SPLM, Silver Peak-Lone Mountain extensional complex.

[6] Due to the lack of numerical dates on offset alluvial landforms in most previous studies, long-term slip-rate estimates vary widely for the DV-FLVFZ in FLV. Estimates of late Pleistocene slip rates range from 1 to 9 mm/yr, indicating that the DV-FLVFZ may accommodate almost none, to essentially all, of the deformation in the northern ECSZ over this time period [*Reheis and Dixon*, 1996; *Reheis and Sawyer*, 1997]. To the south, in northern Death Valley, TCN ^{10}Be and ^{36}Cl geochronology of the offset Red Wall Canyon alluvial fan yields a slip rate of ~4.5 mm/yr (Figure 1) [*Frankel et al.*, 2007]. The right-lateral slip rate along the WMFZ, based on offset alluvial fans dated by TCN ^{36}Cl, is 0.3 to 0.4 mm/yr over late Pleistocene time scales [*Kirby et al.*, 2006].

3. LiDAR and Fault Displacement

[7] The use of high-resolution LiDAR digital topographic data to survey offset alluvial landforms along the DV-FLVFZ is a key part of this study. The LiDAR data were collected with a 33 kHz Optech 2033 ALTM laser source. Point spacing was nominally 1.1 m along-track at nadir, 2.2 m along-track at the scan edge, and 0.73 m cross-track. The flight line spacing was 215 m, which yielded 100% swath overlap, resulting in a shot density of ~3 points/m^2. Individual data points were gridded at 1 m cell size using a kriging algorithm to produce a digital elevation model (DEM) with 1 m horizontal, and 5 to 10 cm vertical, precision [*Shrestha et al.*, 1999]. The DEM was imported into ArcGIS where thalweg positions, and hillshade, slope aspect, and topographic maps were derived from the LiDAR data. We used these data to precisely determine fault offsets at two sites along the northern part of the DV-FLVFZ (Figures 2 and 3; auxiliary material Figure S1).[1]

3.1. Furnace Creek Offset

[8] The Furnace Creek alluvial fan in central FLV is offset right-laterally along two parallel strands of the DV-FLVFZ (Figures 1 and 2). Previous offset estimates for late Pleistocene alluvial fans along this segment of the fault range widely, from 111 m to >550 m [*Brogan et al.*, 1991; *Reheis et al.*, 1995; *Reheis and Sawyer*, 1997]. We used a prominent beheaded channel incised through the fan surface, together with the morphology of the entire fan, to reconstruct the offset Qfio deposit (Figure 2; unit Qfi of *Reheis et al.* [1995]). The hillshaded DEM image, topographic contour map, and channel thalwegs allowed us to accurately restore the offset channel (Figure 2). The slope aspect map aided in the reconstruction of the fan apex as well as the offset channel because it allowed us to highlight subtle topographic features by abrupt changes in slope direction (Figure 2). Based on these data, along with topographic profiles collected across the fan surfaces

[1] Auxiliary material data sets are available at ftp://ftp.agu.org/apend/gl/2007gl030549. Other auxiliary material files are in the HTML.

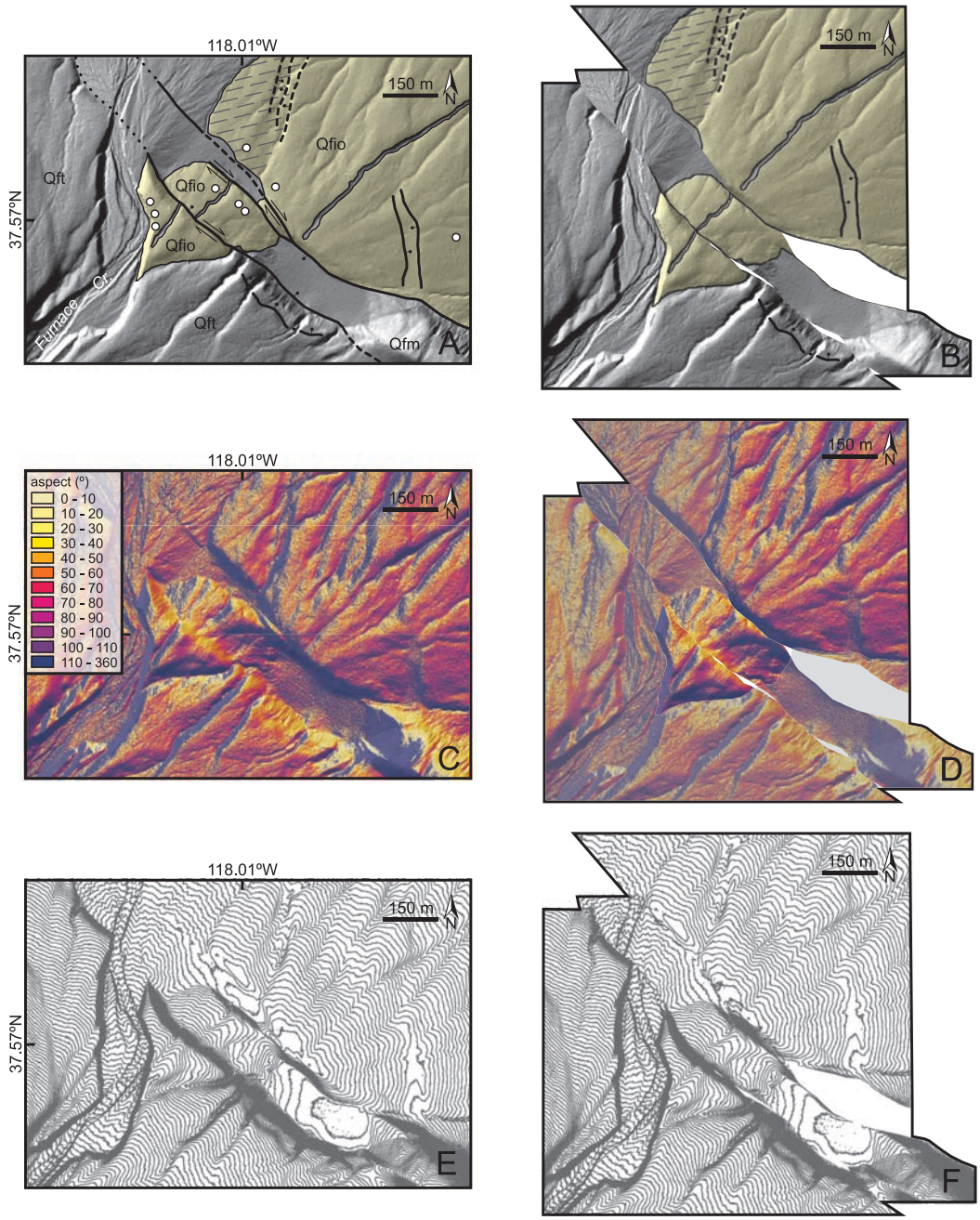

Figure 2. (a) Hillshaded geologic (after *Reheis et al.* [1995]), (c) slope aspect, and (e) topographic maps of the Furnace Creek alluvial fan from LiDAR data (location 2 in Figure 1). (b, d, f)The Furnace Creek fan is retro-deformed 290 ± 20 m based on these data. Hatched pattern in Figures 2a and 2b indicates a fan surface of similar age, but set into the Qfio unit. Contour interval in Figures 2e and 2f is 1 m. White circles in Figure 2a show sample locations.

parallel to the fault (auxiliary material Figures S2 and S3), we determined the late Pleistocene strike-parallel displacement at Furnace Creek to be 290 ± 20 m. The uncertainty in this offset is based on the width of the offset channel. The LiDAR images in Figure 2, particularly the slope aspect map, show this is likely a unique solution to the displacement restoration at this site.

3.2. Indian Creek Offset

[9] Although the Indian Creek fan in northern FLV is deformed by multiple normal faults, the dextral component of offset is largely localized along a single strand (Figures 1 and 3). Late Pleistocene offset at this site was previously estimated at ~122 m, based on the offset of a single abandoned channel [*Reheis et al.*, 1993; *Reheis and Sawyer*, 1997]. Our new data allow a revision of this estimate. Retrodeformation of the Qfiy deposit (unit Qfi of *Reheis et al.* [1993]) on the Indian Creek fan based on the hillshade, slope aspect, and topographic maps, and channel thalwegs allowed us to restore at least four, and possibly six, offset channels incised through the fan surface, in addition to an abrupt change in fan slope direction (Figure 3). Using

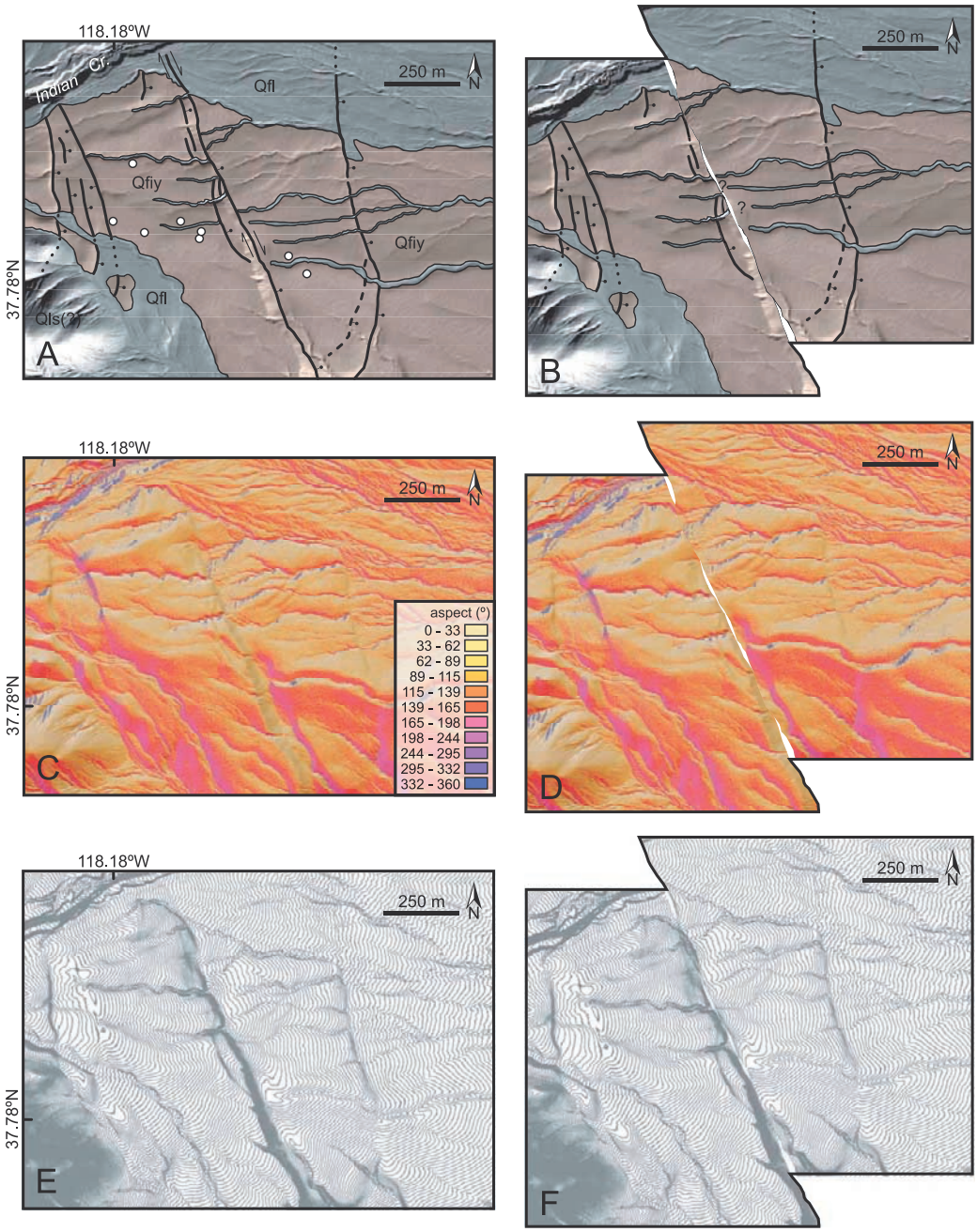

Figure 3. (a) Hillshaded geologic (after *Reheis et al.* [1993]), (c) slope aspect, and (e) topographic maps of the Indian Creek alluvial fan from LiDAR data (location 3 in Figure 1). (b, d, f) The Indian Creek fan is retro-deformed 178 ± 20 m based on these data. Contour interval in Figures 3e and 3f is 1 m. White circles in Figure 3a indicate sample locations.

the average thalweg offsets of four prominent channels on the fan surface, including the channel used by *Reheis et al.* [1993] and *Reheis and Sawyer* [1997], we revise the late Pleistocene displacement at Indian Creek to 178 ± 20 m (Figure 3). The standard deviation of the four offset measurements is 7 m. However, we use a more conservative estimate of 20 m based on channel widths as the uncertainty in our offset measurement.

4. Alluvial Fan Geochronology

[10] We quantified the age of the Furnace Creek and Indian Creek alluvial fans by measuring the concentration of in-situ-produced TCN ^{10}Be in boulders on the fan surfaces [*Lal*, 1991; *Gosse and Phillips*, 2001]. Samples were collected from the top 2 to 5 cm of large boulders on stable parts of fan surfaces mapped as unit Qfi by *Reheis et al.* [1993, 1995] (auxiliary material Figure S4). The offset alluvial fans are characterized by subdued to moderately incised channels, well-developed desert pavement surrounding boulders, moderate to dark coatings of desert varnish on clasts, and a well-developed soil with a 5-to-10-cm-thick, silty vesicular A horizon and an argillic B horizon with moderate clay-film accumulation and stage II to III carbonate development [*Reheis and Sawyer*, 1997].

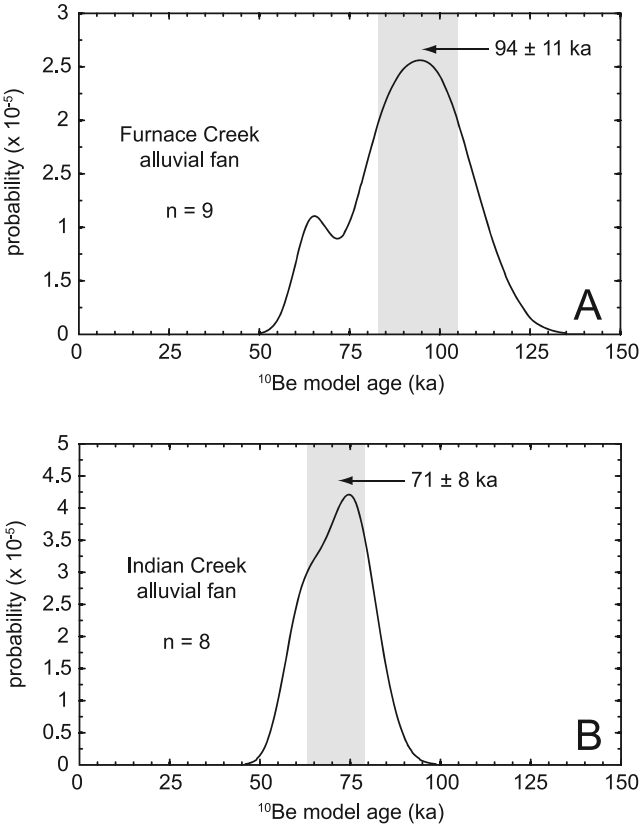

Figure 4. Probability density functions of TCN ^{10}Be ages from the Furnace Creek and Indian Creek alluvial fans in Fish Lake Valley. (a) Furnace Creek fan. Vertical grey bar represents the mean and standard deviation of the eight ages from the Qfio surface (Figure 2) that contribute to the main peak. (b) Indian Creek fan. Vertical grey bar represents the mean and standard deviation of ages from the Qfiy surface (Figure 3).

[11] We measured ^{10}Be/^{9}Be ratios for each sample by accelerator mass spectrometry at Lawrence Livermore National Laboratory. Sample ages were determined from ^{10}Be concentrations with the CRONUS-Earth on-line ^{10}Be-^{26}Al exposure age calculator (Version 1; http://hess.ess.washington.edu/math/), using ^{10}Be production rates based on *Stone* [2000] (auxiliary material Tables S1 and S2).

4.1. Furnace Creek Fan Age

[12] Nine TCN samples were collected from the offset Qfio surface on the Furnace Creek alluvial fan in central FLV (Figure 2). The nine samples range in age from 64 ± 5 ka to 112 ± 8 ka (Figure 4a; auxiliary material Table S1). Eight of the nine samples form a tight cluster of ages in the probability distribution in Figure 4a. The distribution of these eight samples is taken as evidence that the fan surface has remained relatively stable and that the samples have been exposed to cosmic rays in their current configuration since deposition. The youngest sample is clearly an outlier (Figure 4a), and after reexamination of the sample location, we think this boulder was recently exhumed from the eroded southwestern edge of the alluvial fan. We therefore take the age of the fan to be the mean and standard deviation of the remaining eight samples, which yields an age of 94 ± 11 ka (Figure 4a). This age falls near the middle of the 50 to 130 ka age estimated by *Reheis and Sawyer* [1997] for the Furnace Creek fan on the basis of soil development and surface morphology.

4.2. Indian Creek Fan Age

[13] At the Indian Creek alluvial fan we collected eight TCN samples from the displaced Qfiy surface (Figure 3). The samples range in age from 59 ± 4 ka to 81 ± 6 ka (Figure 4b; auxiliary material Table S2). Although somewhat younger, the samples from Indian Creek exhibit a strong, single peak similar to the Furnace Creek data, as shown in the probability distribution in Figure 4b. As with the Furnace Creek samples, we take this to indicate that the boulders share a similar exposure history and have remained at the surface in their present geometry since deposition. The relatively tight cluster of ages yields a mean age and standard deviation of 71 ± 8 ka, which we take as the age of the Indian Creek alluvial fan (Figure 4b). This age agrees well with the previously reported age of 50 to 130 ka estimated on the basis of soil development and surface morphology [*Reheis and Sawyer*, 1997].

5. Fault Slip Rates

[14] The TCN ^{10}Be exposure ages from the surfaces of the Furnace Creek and Indian Creek alluvial fans are interpreted to be maximum ages with regard to calculating slip rates because the incised, offset channels must have formed at some unconstrained time after deposition. In addition, our rates do not take into account extensional faulting along the western White Mountains piedmont or potential off-fault deformation. As such, the slip rates reported here should be interpreted as minima, although we are confident that we have captured nearly all of the right-lateral displacement along the fault zone.

[15] Combining the 290 ± 20 m of offset at Furnace Creek with the 94 ± 11 ka age of the offset Qfio surface yields a slip rate of 3.1 ± 0.4 mm/yr in central FLV. This rate is within the broad range of 1.5 to 9.3 mm/yr estimated by *Reheis and Sawyer* [1997] for this site. A slightly slower slip rate of 2.5 ± 0.4 mm/yr results from the 178 ± 20 m offset of a 71 ± 8 ka old surface at Indian Creek in northern FLV. Previous slip rate estimates at this site ranged from 1.1 to 3.3 mm/yr [*Reheis and Sawyer*, 1997].

6. Implications for ECSZ Strain Distribution

[16] Previous work suggests that as strain is transferred from the Owens Valley and Panamint Valley-Hunter Mountain-Saline Valley faults, via down-to-the-northwest normal faults, into FLV, rates of deformation should increase on the NW-trending, northern DV-FLVFZ [*Dixon et al.*, 1995, 2000; *Reheis and Dixon*, 1996; *Lee et al.*, 2001]. In contrast, our results show that slip rates on the DV-FLVFZ actually decrease northward. The geologic rate for the DV-FLVFZ from the dextrally offset Red Wall Canyon fan in northern Death Valley, measured over a similar time scale, is ~4.5 mm/yr (^{10}Be dates yield a minimum slip rate of >4.2 +1.9/−1.1 mm/yr; ^{36}Cl geochronology provides a rate of 4.7 +0.9/−0.6 mm/yr) [*Frankel et al.*, 2007]. To the north, in FLV, this rate slows to ~2.5 to 3 mm/yr.

[17] Moreover, taking into account the 0.3 to 0.4 mm/yr late Pleistocene right-lateral slip rate of the WMFZ [*Kirby et al.*, 2006], the total long-term rate of deformation accommodated by the two major faults at ~37.5°N is less than 4 mm/yr of the 9.3 ± 0.2 mm/yr region-wide rate of dextral shear determined from geodesy [*Bennett et al.*, 2003]. This implies that either: (1) deformation at the latitude of FLV is accommodated by structures other than the DV-FLVFZ and WMFZ; or (2) the region is currently experiencing a strain transient similar to that in the Mojave segment of the ECSZ [e.g., *Oskin and Iriondo*, 2004].

[18] If strain rates have remained constant during the late Pleistocene and Holocene, as has been suggested at the latitude of northern Death Valley [*Frankel et al.*, 2007], then approximately half of the total strain budget in the northern ECSZ must be accommodated off of the two main faults, either through Long Valley caldera [e.g., *Kirby et al.*, 2006] or to the east of FLV. Given the northward decrease in slip rate along the DV-FLVFZ documented here, we suspect that most of the strain is accommodated to the east. *Oldow et al.* [1994] and *Petronis et al.* [2002] demonstrated that faults east of FLV (Figure 1) acted as extensional transfer zones and accommodated vertical axis block rotation between the nascent DV-FLVFZ and Walker Lane from the mid-Miocene through the Pliocene. Our results suggest these structures may still play an important role in accommodating strain transfer from the ECSZ to the active faults of the Walker Lane in western Nevada. In particular, the ~2.5 mm/yr rate from the Indian Creek fan implies that the Emigrant Peak fault accommodates ≥0.5 mm/yr of elastic strain, in agreement with the late Pleistocene rate of 0.4 to 1.3 mm/yr estimated for this fault [*Reheis and Sawyer*, 1997].

[19] If true, the ECSZ-Walker Lane transition zone must begin south of the Mina deflection, from the Emigrant Peak fault zone through the Silver Peak-Lone Mountain extensional complex [*Oldow et al.*, 1994] in a broader, more diffuse zone than previously recognized (Figure 1). As the ECSZ and Walker Lane become a more structurally mature component of the Pacific-North America plate boundary, strain may localize on individual structures such as the DV-FLVFZ in FLV and the WMFZ in Owens Valley [e.g., *Faulds et al.*, 2005; *Wesnousky*, 2005]. It appears, however, that since at least the late Pleistocene, and likely earlier, the northernmost part of the ECSZ may have accommodated deformation in a zone spanning a width of >100 km from Owens Valley in the west to the western margin of the Great Basin east of FLV.

[20] **Acknowledgments.** This study was funded by NSF grants EAR-0537901, EAR-0537580, and EAR-0538009, a NASA Earth System Science Fellowship, a LLNL UEPP Fellowship, and assistance from the U.S. Department of Energy (UC-LLNL contract W-7405-Eng-48). LiDAR data were collected by NCALM. T. Dixon and J. Oldow provided thoughtful reviews.

References

Bennett, R. A., B. P. Wernicke, N. A. Niemi, A. M. Friedrich, and J. L. Davis (2003), Contemporary strain rates in the northern Basin and Range province from GPS data, *Tectonics*, *22*(2), 1008, doi:10.1029/2001TC001355.

Brogan, G. E., K. S. Kellog, D. B. Slemmons, and C. L. Terhune (1991), Late Quaternary faulting along the Death Valley-Furnace Creek fault system, California and Nevada, *U.S. Geol. Surv. Bull.*, *1991*, 23 pp.

Dixon, T. H., S. Robaudo, J. Lee, and M. C. Reheis (1995), Constraints on present-day Basin and Range deformation from space geodesy, *Tectonics*, *14*, 755–772.

Dixon, T. H., M. Miller, F. Farina, H. Wang, and D. Johnson (2000), Present-day motion of the Sierra Nevada block and some tectonic implications for the Basin and Range province, North American Cordillera, *Tectonics*, *19*, 1–24.

Dixon, T. H., E. Norabuena, and L. Hotaling (2003), Paleoseismology and Global Positioning System: Earthquake-cycle effects and geodetic versus geologic fault slip rates in the eastern California shear zone, *Geology*, *31*, 55–58.

Faulds, J. E., C. D. Henry, and N. H. Heinz (2005), Kinematics of the northern Walker Lane: An incipient transform fault along the Pacific-North America plate boundary, *Geology*, *33*, 505–508.

Frankel, K. L., et al. (2007), Cosmogenic ^{10}Be and ^{36}Cl geochronology of offset alluvial fans along the northern Death Valley fault zone: Implications for transient strain in the eastern California shear zone, *J. Geophys. Res.*, *112*, B06407, doi:10.1029/2006JB004350.

Gosse, J. C., and F. M. Phillips (2001), Terrestrial in situ cosmogenic nuclides: Theory and application, *Quat. Sci. Rev.*, *20*, 1475–1560.

Kirby, E., D. W. Burbank, M. Reheis, and F. Phillips (2006), Temporal variations in slip rate of the White Mountain Fault Zone, eastern California, *Earth. Planet. Sci. Lett.*, *248*, 153–170, doi:10.1016/j.epsl.2006.05.026.

Lal, D. (1991), Cosmic ray labeling of erosion surfaces: In situ nuclide production rates and erosion models, *Earth. Planet. Sci. Lett.*, *104*, 424–439.

Lee, J., C. M. Rubin, and A. Calvert (2001), Quaternary faulting history along the Deep Springs fault, California, *Bull. Geol. Soc. Am.*, *113*, 855–869.

Oldow, J. S., G. Kohler, and R. A. Donelick (1994), Late Cenozoic extensional transfer in the Walker Lane strike-slip belt, Nevada, *Geology*, *22*, 637–640.

Oskin, M., and A. Iriondo (2004), Large-magnitude transient strain accumulation on the Blackwater fault, eastern California shear zone, *Geology*, *32*, 313–316.

Petronis, M. S., J. W. Geissman, J. S. Oldow, and W. C. McIntosh (2002), Paleomagnetic and ^{40}Ar/^{39}Ar geochronologic data bearing on the structural evolution of the Silver Peak extensional complex, west-central Nevada, *Bull. Geol. Soc. Am.*, *114*, 1108–1130.

Reheis, M. C., and T. H. Dixon (1996), Kinematics of the eastern California shear zone: Evidence for slip transfer from Owens and Saline Valley fault zones to Fish Lake Valley fault zone, *Geology*, *24*, 339–342.

Reheis, M. C., and T. L. Sawyer (1997), Late Cenozoic history and slip rates of the Fish Lake Valley, Emigrant Peak, and Deep Springs fault zones, Nevada and California, *Bull. Geol. Soc. Am.*, *109*, 280–299.

Reheis, M. C., T. L. Sawyer, J. L. Slate, and A. R. Gillispie (1993), Geologic map of late Cenozoic deposits and faults in the southern part of the Davis Mountain 15' quadrangle, Esmeralda County, Nevada, *U.S. Geol. Surv. Map*, *I-2342*.

Reheis, M. C., J. L. Slate, and T. L. Sawyer (1995), Geologic map of late Cenozoic deposits and faults in parts of the Mt. Barcroft, Piper Peak, and Soldier Pass 15' quadrangles, Esmeralda County, Nevada, and Mono County, California, *U.S. Geol. Surv. Map*, *I-2464*.

Shrestha, R. L., W. E. Carter, M. Lee, P. Finer, and M. Sartori (1999), Airborne laser swath mapping: Accuracy assessment for surveying and mapping applications,, *Surv. Land Inf. Sci..*, *59*, 83–94.

Stone, J. O. (2000), Air pressure and cosmogenic isotope production, *J. Geophys. Res.*, *105*, 23,753–23,759.

Wesnousky, S. G. (2005), The San Andreas and Walker Lane fault systems, western North America: Transpression, transtension, cumulative slip and the structural evolution of a major transform plate boundary, *J. Struct. Geol.*, *27*, 1505–1512.

J. F. Dolan, Department of Earth Sciences, University of Southern California, 3651 Trousdale Parkway, Los Angeles, CA 90089, USA. (dolan@usc.edu)

R. C. Finkel, Center for Accelerator Mass Spectrometry, Lawrence Livermore National Laboratory, P.O. Box 808, 7000 East Avenue, Livermore, CA 94550, USA. (finkel1@llnl.gov)

K. L. Frankel, School of Earth and Atmospheric Sciences, Georgia Institute of Technology, 311 Ferst Drive, Atlanta, GA 30332, USA. (kfrankel@usc.edu)

J. S. Hoeft, William Lettis & Associates, Inc., 1777 Botelho Drive, Suite 262, Walnut Creek, CA 94596, USA. (jeffhoeft@gmail.com)

L. A. Owen, Department of Geology, University of Cincinnati, P.O. Box 0013, Cincinnati, OH 45221, USA. (lewis.owen@uc.edu)